Invariant-mass dependence of two-pion inclusive correlation functions

E. L. Berger, R. Singer, and G. H. Thomas
High Energy Physics Division, Argonne National Laboratory, Argonne, Illinois 60439*

T. Kafka
State University of New York,† Stony Brook, New York 11794

(Received 4 August 1976)

We study high-energy two-particle inclusive correlations as a function of the invariant mass M of the pair. Using data from 205-GeV/c pp interactions, we compare the correlation functions $C(M)$ for $(+-)$ and $(--)$ pairs of produced pions. Strong positive correlations are observed in both distributions in the form of a broad threshold enhancement at small M. The decrease of $C(M)$ as M increases is interpreted in the Mueller-Regge framework. From the M dependence of C^{+-} we extract an effective-trajectory intercept of roughly $\alpha(0)\simeq 0.5\pm 0.1$, consistent with the (ρ,f) pair. For the exotic $(--)$ system, we find a low intercept, $\alpha(0)\simeq -0.5$. A ρ-resonance signal is observed above background in $C^{+-}(M)$. Near threshold, effects suggestive of Bose symmetry are seen but are not conclusive. In an exclusive picture, we relate most of the correlation in the threshold region to resonances involving three or more pions. We also examine the joint correlations in M and the azimuthal angle ϕ.

I. INTRODUCTION

The experimental study of two-particle inclusive distributions in high-energy interactions has deepened our understanding of multiparticle production processes.[1] The two-particle inclusive correlation function is observed to be roughly energy independent in the central region of rapidity space and to decrease rapidly in magnitude as the rapidity interval widens between the two particles. These features are characteristic properties of models, such as the ABFST multiperipheral scheme[2] and the Mueller-Regge ansatz,[3] which are built on the principle of short-range order. Phenomenological approaches have been devised to interpret the magnitude and rapidity dependence of the correlation functions. Popular are prescriptions in which the production and subsequent decay of clusters are deemed responsible.[4] The data are used to determine certain properties of the clusters.[4,5] This interpretation provides a convenient though enigmatic summary of a large body of data. One important question which remains unsettled is the extent to which only those concepts familiar from low-multiplicity exclusive investigations suffice for the understanding of multihadron processes. These include the notions of perpheral t-channel exchanges at large invariant mass, resonance dominance at low invariant mass, and the qualitatively successful duality principle.

In most investigations of inclusive correlations, the *rapidity* variable y is used. This procedure is well motivated when the only aim is to test the concept of short-range order. Experimentally, in situations in which angles and not momenta are measured, it is the only available variable [$y \simeq \ln\tan(\theta/2)$]. For more detailed investigations of the correlations, rapidity may be seriously disadvantageous. In this article, we study inclusive correlations $C(M)$ as functions of the *invariant mass* M of the two-particle system. Data from the ANL–Fermilab–Stony Brook 205-GeV/c pp experiment[6] are used to calculate $C^{+-}(M)$ and $C^{--}(M)$ for $(+-)$ and $(--)$ pairs of pions. We find important structure in $C(M)$ in both cases, and we discuss its significance.

There are evident arguments in favor of mass as a dynamical variable. Singularities such as resonances and thresholds appear at fixed values of mass. Bose-Einstein interference effects are expected to depend on the square of the difference of the four-vector momenta of identical bosons, $(p_1-p_2)^2=4m_\pi^2-M^2$. Regge and duality properties of the four-to-four forward Mueller amplitude, which represents the correlation function, are functions of the two-particle invariant mass. To be sure, at large mass rapidity separation and mass are related simply, because in this limit

$$\Delta y \sim \ln M^2 .$$

However, because the relationship between $C(\Delta y)$ and $C(M)$ involves an integral over the transverse momenta, possible important structure in the data at small M will be smeared when viewed in terms of Δy. The correlation function $C(\Delta y)$ is itself observed to be large at small $|\Delta y|$ ($\lesssim 1$). The interpretation of this structure in terms of resonances (or other forms of clustering) with relatively low mass may be more readily checked by

examination of $C(M)$. Invariant mass has long been a useful variable in high-energy investigations. Its disuse in high-multiplicity processes is explained in part by the large combinatorial background present in the two-particle density $(1/\sigma)d\sigma/dM$. We argue that the correlation function removes the uncorrelated background.

In Sec. II, we define the two-particle inclusive correlation function $C(M)$ and discuss its dependence on the invariant mass M. Using data[6] on $pp \to \pi^+\pi^- X$ and $pp \to \pi^-\pi^- X$ at 205 GeV/c, we examine the correlation functions $C^{+-}(M)$ and $C^{--}(M)$ for $(+-)$ and $(--)$ pairs of pions. Strong positive correlations in the form of broad peaks near the two-pion threshold are observed in both distributions. As M increases, $C_2^{--}(M)$ drops more rapidly than $C_2^{+-}(M)$. A ρ-resonance signal is visible above the background in $C_2^{+-}(M)$. The possibility of Bose-Einstein interference phenomena is investigated near threshold in $C_2^{--}(M)$. Finally, we examine the dependence of the correlation function $C(M,\phi)$ on the relative azimuthal angle ϕ between the transverse-momentum vectors of the two pions.

In Sec. III, we show that the rate of decrease of $C_2^{+-}(M)$ is consistent with an inclusive Mueller-Regge exchange picture in which the M dependence is controlled by the (ρ,f) pair of trajectories. The faster fall of $C_2^{--}(M)$ agrees with duality expectations and would require a low-lying trajectory with intercept $\alpha_E(0) \simeq -0.5$. In an exclusive framework developed in Sec. IIIC, we interpret the background below the ρ and most of the threshold structure as reflections of decay from resonant systems of three or more hadrons. Our conclusions and perspective are summarized in Sec. IV. In Appendix A some details are presented of the way we treat the data.

II. CORRELATION FUNCTIONS IN INVARIANT MASS

A. Preliminaries

The definition of the two-particle inclusive correlation function is

$$C_2(p_1,p_2) \equiv \rho_2(p_1,p_2) - \rho_1(p_1)\rho_1(p_2) \ . \tag{2.1}$$

In this expression, p_1 and p_2 are the momenta of the two hadrons. The two-particle density is

$$\rho_2(p_1,p_2) \equiv \frac{E_1E_2}{\sigma}\frac{d^2\sigma}{d^3p_1 d^3p_2} \ . \tag{2.2}$$

The single-particle inclusive density is

$$\rho_1(p) = \frac{E}{\sigma}\frac{d\sigma}{d^3p} \ . \tag{2.3}$$

The cross section σ appearing in Eqs. (2.2) and (2.3) is taken to be the inelastic cross section. When discussing the data we shall comment on effects arising from other choices.

The function $C_2(p_1,p_2)$ in Eq. (2.1) is a function of six independent variables. A common choice for these six is: the total c.m. energy $\sqrt{s}$, the c.m. rapidities y_1 and y_2 of the two hadrons, the magnitudes p_{T1} and p_{T2} of the two transverse momenta, and ϕ, the relative azimuthal angle between $\vec{p}_{T1}$ and $\vec{p}_{T2}$. In models with pure short-range order, these six variables reduce to four: $\Delta y = (y_1 - y_2)$, p_{T1}, p_{T2}, and ϕ. For reasons stated in the Introduction, we advocate including the invariant mass M of the two-particle system as an independent variable. Because interesting structure[7] has been observed at small Δy in the ϕ distribution, we retain the ϕ variable as well as p_{T1} and p_{T2} in our set. To complete the set, we add $\sqrt{s}$ and one other variable to locate the longitudinal position of the system with mass M. This last variable need not be specified since we integrate over it. A possible choice is the rapidity $y_{\pi\pi}$ of the system. The relationship between M and Δy is

$$M^2 = 2m_\pi^2 - 2\vec{p}_{T1}\cdot\vec{p}_{T2} + 2m_{T1}m_{T2}\cosh(\Delta y) \tag{2.4}$$

with

$$m_T^2 = m_\pi^2 + p_T^2 \ .$$

Equation (2.4) shows that

$$M^2 \propto \exp(|\Delta y|) \ ,$$

for large M and $|\Delta y|$. However, at small M or Δy, the relationship between these variables is influenced greatly by the values of p_{T1} and p_{T2}. If the transverse momenta are integrated over, the effect is to smear possible structure in M or in Δy when viewed in terms of the other variable.

After integrating Eq. (2.1) over the p_T and ϕ dependences, and over the longitudinal position of the pair, we obtain a correlation distribution which is a function of M only (at fixed $\sqrt{s}$). We then have

$$C_2(M) = \rho_2(M) - \rho_1 \otimes \rho_1(M) \ . \tag{2.5}$$

In Eq. (2.5), $\rho_2(M)$ is the usual differential cross section $d\sigma/dM$, divided by σ_{inel}. The second term represents the combinatorial background which we subtract from ρ_2 to obtain $C_2(M)$. This product of single-particle distributions at fixed pair mass is

$$\rho_1 \otimes \rho_1(M) = \int \frac{d^3p_1}{E_1}\frac{d^3p_2}{E_2}\,\delta([(p_1+p_2)^2]^{1/2} - M) \times \rho_1(p_1)\rho_1(p_2) \ . \tag{2.6}$$

In Appendix A, we describe how the data for

$\rho_1 \otimes \rho_1$ are expressed numerically as a function of M.

B. Data

The data discussed in this section were obtained from the Argonne–Fermilab–Stony Brook analysis of an exposure of 205-GeV/c protons in the 30-inch hydrogen bubble chamber at Fermilab. Details of the experiment have been published elsewhere.[6] The data consist of an inclusive sample of 5128 inelastic events. All negative tracks are assumed to be negative pions. Positive tracks except for those clearly identified as protons by ionization are assumed to be positive pions. In addition, a positive track with $x>0.6$ is assumed to be a proton.

In Fig. 1 the three distributions $\rho_2(M)$, $\rho_1 \otimes \rho_1(M)$, and $C_2(M)$ are presented as functions of the two-pion invariant mass. Figures 1(a) and 1(b) show the results for $\pi^+\pi^-$ and $\pi^-\pi^-$, respectively. No selection is made on the location in phase space of the pair. The mass distributions extend to very high values of M, but we concentrate here on the region $M \lesssim 2$ GeV. We present the data in 40-MeV bins; the average mass resolution is about 20 MeV for pions in the central region of rapidity.

It is useful to examine first the $(--)$ data, since no resonancelike structure is expected.[8] The distributions $\rho_2(M)$ and $\rho_1 \otimes \rho_1(M)$ are indeed rather smooth. Both show broad enhancements extending

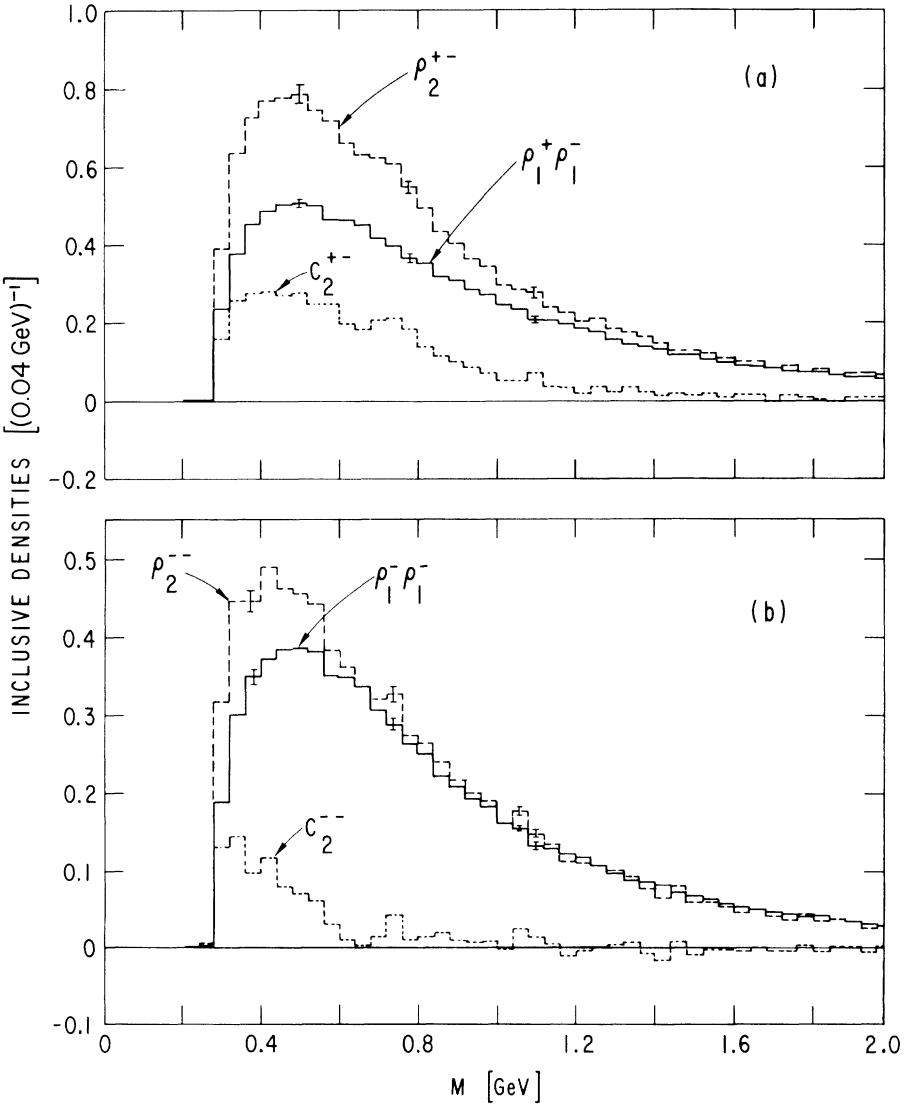

FIG. 1. Displayed as a function of dipion invariant mass are the three distributions ρ_2, $\rho_1 \otimes \rho_1$, and C_2 for (a) $\pi^+\pi^-$ pairs and (b) $\pi^-\pi^-$ pairs from $pp \to \pi\pi X$ at 205 GeV/c.

from threshold to ~1 GeV. The curves are remarkably similar in shape and magnitude above 0.6 GeV, but differ in the region $M < 0.6$ GeV. The correlation function $C_2^{--}(M)$ shows structure next to the two-pion threshold, with width of ≈ 200 MeV, and it is nearly zero for $M > 0.6$ GeV. That $C_2^{--}(M)$ is featureless within statistics for all $M \gtrsim 0.6$ GeV conforms to expectations that the exotic $\pi^-\pi^-$ system should show no strong correlations. The roughly constant value of $C_2^{--}(M) \approx 0$ above 0.6 GeV also confirms that our definition of the correlation function is reasonable. Changes, for example, in the normalizing cross section in Eqs. (2.2) and (2.3) from σ_{inel} to σ_{tot} change the level of $\rho_1 \otimes \rho_1$ by ~20–30% relative to ρ_2 but do not change M dependences. The structure in $C_2^{--}(M)$ below 0.6 GeV is striking. We return to a discussion of its origins below, in Secs. II B 2 and III.

The data for $(+-)$ combinations are shown in Fig. 1(a). The distribution $\rho_1^+ \otimes \rho_1^-$ is again smooth, whereas ρ_2^{+-} shows structure in the ρ region.[9] The two curves do not coincide, in contrast to $(--)$, until $M \gtrsim 1.6$ GeV. Because of their different dependence on M, ρ_2^{+-} and $\rho_1^+ \otimes \rho_1^-$ cannot be brought into coincidence in the region $0.6 \lesssim M \lesssim 1.6$ GeV except through an unmotivated M-dependent multiplicative factor. The function $C_2^{+-}(M)$ shown in Fig. 1(a) has a broad enhancement extending from threshold to ~1.0 GeV, on which is superimposed a peak which we identify with the ρ meson.

In Fig. 2, we compare $C_2(M)$ for $(+-)$ and $(--)$ pairs. We note that $C_2^{+-}(M)$ and $C_2^{--}(M)$ differ in magnitude and behave differently as functions of M, whereas the differences in ρ_2^{+-} and ρ_2^{--} are not readily apparent (Fig. 1). This demonstrates the virtue of removing the large combinatorial background.

The integral of the two-particle correlation function is the second Mueller moment

$$f_2 = \int C_2(M)dM \ .$$

When the M range extends over the full spectrum, we obtain the value[6] $f_2^{--} = 0.8 \pm 0.1$. For $M \lesssim 0.6$ GeV, $f_2^{--} = 0.7 \pm 0.1$. Thus the low-mass peak in $(--)$ accounts for $\approx 90\%$ of the full f_2^{--}. For all M we find $f_2^{+-} = 4.0 \pm 0.2$, whereas for $M \lesssim 0.6$ the value is $f_2^{+-} = 2.0 \pm 0.1$, or 50% of the total. (As remarked above, we have excluded identifiable protons from our sample; thus, the value of f_2^{+-} quoted here differs from the value published previously[6]).

The contrast between $(--)$ and $(+-)$ in Fig. 2 may be compared with the similarity in shape[1] of $C_2^{+-}(\Delta y)$ and $C_2^{--}(\Delta y)$. In rapidity, the correlation functions differ to first approximation only in normalization; this is associated with the fact that

$$f_2^{+-} = f_2^{--} + \langle n_- \rangle \ .$$

The structure in $C_2^{--}(M)$ at small M in Fig. 2 corresponds to the peak at $\Delta y = 0$ in $C_2^{--}(\Delta y)$. For $(+-)$, a much broader spectrum of mass values provides the peak in $C^{+-}(\Delta y)$ at $\Delta y = 0$.

1. Resonance contributions

The ρ signal in Fig. 2 is observed on a rapidly falling background. The difference of the shapes of the $(+-)$ and $(--)$ curves argues against using the $(--)$ curve as background. Fitting the $(+-)$ distribution with the sum of a Breit-Wigner formula plus a noninterfering quadratic background over the range $0.5 \leq M \leq 1.0$ GeV, we obtain directly the mean number of neutral ρ's per inelastic event:

$$\langle n_{\rho 0} \rangle = 0.30 \pm 0.04 \ .$$

The χ^2 of this fit is 14.4 for 9 degrees of freedom. The mass and width were fixed at $M_{\rho 0} = 0.748$ GeV and $\Gamma_\rho = 0.128$ GeV.[10] This value of $\langle n_{\rho 0} \rangle$ may be compared with the value 0.33 ± 0.06 obtained previously[9] from a fit to $\rho_2^{+-}(M)$.

No resonance signal is seen above the smooth background in the f- and g-meson regions. For a very crude upper bound on f production, we may take all events in C_2^{+-} in the interval $M = 1.26$ GeV $\pm \Gamma/2$, with $\Gamma = 0.15$ GeV. We obtain $\langle n_f \rangle / \langle n_\rho \rangle < 0.3/\frac{2}{3} = 0.45$. The factor $\frac{2}{3}$ is the branching ratio of the f into $\pi^+\pi^-$. Similarly, for the g, we take $M = 1.68$ GeV $\pm \Gamma/2$ with $\Gamma = 0.18$ GeV, and obtain $\langle n_g \rangle / \langle n_\rho \rangle < 0.15/\frac{1}{4} = 0.6$. These numbers are unreasonably large. They would be reduced by at least $\frac{1}{3}$ if one were to take the same resonance-

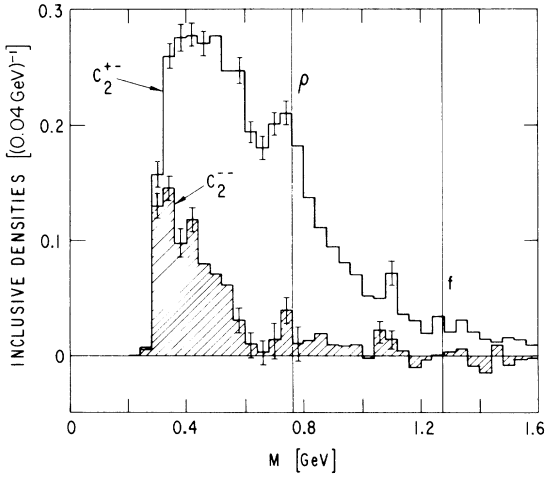

FIG. 2. The correlation functions $C_2(M)$ are displayed versus dipion invariant mass. Shown are results for $(+-)$ and $(--)$ pairs. The nominal locations of the ρ ($M = 0.76$ GeV) and f ($M = 1.27$ GeV) are marked.

to-background ratio which we observe in the ρ region.

2. Broad threshold structure

Threshold enhancements are present in both $C_2^{+-}(M)$ and $C_2^{--}(M)$. They differ appreciably in overall magnitude, and to some extent in the details of their mass dependences. In the next two subsections (3 and 4) we attempt to parametrize these differences quantitatively, and we comment on the interpretation of the enhancements.

Some structure near threshold in both C_2^{+-} and C_2^{--}, as well as a broad background under the ρ in C_2^{+-} may be anticipated as a result of the decay of resonances with multiplicity $m > 2$, e.g., η, ω, A_2, g. These decays produce correlated but generally nonresonant pairs of $\pi^+\pi^-$ and $\pi^-\pi^-$. Their effects are not removed from C_2. In Sec. III C we provide a formal analysis of C_2 from an exclusive point of view, which allows us to relate the threshold structure to the properties of resonances with decay multiplicity $m \geq 3$. However, this exclusive approach does not explain naturally the fact that $C_2^{--}(M)$ is observed to decrease with M more rapidly than $C_2^{+-}(M)$. Indeed, the exclusive argument would suggest "backgrounds" of similar shape in both C_2^{+-} and C_2^{--} near, e.g., $M = 0.76$ GeV, the ρ location. In Sec. III, using the Mueller-Regge inclusive framework, we interpret the suppression of C_2^{--} as a natural consequence of duality requirements.

3. Interference phenomena near threshold

In addition to the contribution from higher-multiplicity resonance decay, other effects influence the M dependence of $C_2(M)$ near threshold. For example, we recall the peak near threshold in the $\pi^-\pi^-$ mass distribution observed in the annihilation process $\bar{p}n \to \pi^+\pi^-\pi^-$. A dynamical interpretation of this was given by Lovelace.[11] In his model, resonances are present only in the two $\pi^+\pi^-$ channels. The structure at low mass in the $\pi^-\pi^-$ distribution is a reflection of both identical-particle symmetry and dynamical ingredients in his amplitude. Thus, there are at least two effects which contribute to the threshold enhancement in the inclusive function $C_2(M)$: reflections of resonance decay and the Bose-Einstein identical-boson symmetry property of production amplitudes. We shall conclude that we find no reliable means to disentangle these two influences in the data sample.

The influence of Bose-Einstein statistics on the distribution of like pions with small relative momenta has been studied by several groups.[12] A standard assumption made is that in some properly chosen variable the $\pi^-\pi^-$ distributions should show substantially different behavior from $\pi^+\pi^-$ distributions. With all other effects neglected, one expects an enhancement of the dipion yield for like pions relative to unlike pions when the four-momenta p_1 and p_2 are equal. If $\Delta = -(p_1 - p_2)^2$, the effect is expected at and near $\Delta = 0$. Because $\Delta = M^2 - 4m_\pi^2$, we investigate the threshold region in $C(M)$.

Certain small differences are indeed apparent in the mass dependences of $C_2^{+-}(M)$ and $C_2^{--}(M)$ near threshold. As seen in Fig. 2, the threshold peak in $C_2^{+-}(M)$ is centered near 450 MeV, whereas in C_2^{--} it occurs below 400 MeV. Correspondingly, in the lowest mass bin ($2m_\pi \leq M \leq 2m_\pi + 40$ MeV) the value of C_2^{--} is relatively greater than C_2^{+-}. This effect may be restated in a more quantitative fashion.

We propose now to examine the normalized correlation function

$$R(M) = C_2(M)/\rho_1 \otimes \rho_1(M) \ .$$

The uncorrelated products of the single-pion densities $\rho_1^+ \otimes \rho_1^-(M)$ and $\rho_1^- \otimes \rho_1^-(M)$ have similar dependence on M, but they differ in normalization because there are more π^+ than π^- in the data sample. Therefore, in dividing $C_2(M)$ by $\rho_1 \otimes \rho_1$, we change the relative normalization of the $(+-)$ and $(--)$ correlation distributions, but not their relative mass dependence.

Values of $R(M)$ are presented in Table I. Whereas $C_2^{+-}(M)$ is roughly a factor of 2 larger than $C_2^{--}(M)$ in the near-threshold region, the values of R^{+-} and R^{--} are more nearly equal. For $M \leq 0.42$ GeV, an interval which extends one pion mass above threshold, we find $R^{+-} = 0.64 \pm 0.03$ and $R^{--} = 0.42 \pm 0.03$. Thus, relative to the uncorrelated measure, the $(--)$ system appears to peak less toward threshold than does $(+-)$. However, subdividing the data into 40-MeV bins, we find a clear variation of R^{--} over the range $M = 0.28$

TABLE I. Ratio $C_2/\rho_1 \otimes \rho_1$ as a function of invariant mass.

M (GeV)	R^{+-}	R^{--}
	(a)	
0.28–0.32	0.67 ± 0.07	0.68 ± 0.07
0.32–0.36	0.68 ± 0.03	0.48 ± 0.03
0.36–0.40	0.61 ± 0.03	0.28 ± 0.04
0.40–0.44	0.57 ± 0.04	0.32 ± 0.04
	(b)	
0.28–0.42	0.64 ± 0.03	0.42 ± 0.03
0.42–0.64	0.51 ± 0.03	0.15 ± 0.03
0.64–0.86	0.45 ± 0.03	0.06 ± 0.01

to 0.44 GeV. These results are presented in Table I(a). Little variation is seen in R^{+-} over the same M interval. We observe that R^{--} falls by roughly one-half from threshold to $M = 0.42$ GeV. If we take this variation to be entirely a manifestation of Bose-Einstein effects, we find that the dimension in M over which symmetry effects are important is of order m_π. However, we cannot exclude the possibility that some or all of this variation is due to other effects which also contribute to the threshold structure.

C. Joint correlations

As remarked in Sec. II A, the inclusive correlation function depends in general on six variables: $\sqrt{s}$, M, p_{T1}, p_{T2}, ϕ, and $y_{\pi\pi}$. Further insight may be gained by studying the s and M dependences of C_2 for restricted values of the four other variables. In this context, an investigation of the semi-inclusive distribution $C_2^{(n)}(M)$ for fixed charge multiplicity might be instructive. Here we limit ourselves to a presentation of $C_2(M, \phi)$.

Structure in the distribution of the azimuthal-angle variable was previously observed to be particularly strong at small Δy.[7] It was suggested that this behavior at small ϕ could be due to Bose-Einstein statistics.[7] One obvious difficulty with this interpretation is that no restrictions were imposed on the p_T values in these previous analyses. Thus, the peak in ϕ may be due to pairs for which the two p_T values are substantially different; such a situation does not satisfy the Bose-Einstein condition. By limiting M to be small, we are assured that the two four-momentum vectors do not differ greatly. This is an additional advantage of the M variable.

To begin, we examine the distributions ρ_2, $\rho_1 \otimes \rho_1$, and C_2 as functions of M for various selections on the azimuthal angle. In Fig. 3, we present $C_2^{+-}(M)$ for three intervals of ϕ. Data for $C_2^{--}(M)$ are shown in Fig. 4. For both (+ −) and (− −) there is a strong positive correlation between small M and $|\phi| < 45°$. The curves for $\phi > 135°$ are suppressed near threshold. For (+ −), events in the ρ region stand out more clearly in this latter distribution.[8]

The enhancement near $\phi = 0$ for small M is at least partially kinematical in origin. For given values of the overall c.m. momenta of the two pions, a smaller value of mass is obtained if the

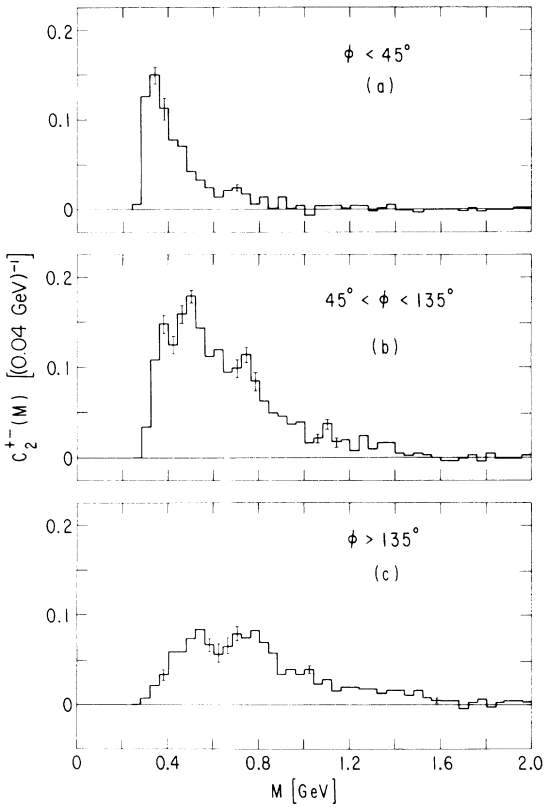

FIG. 3. The joint correlation function $C_2^{+-}(M, \phi)$ is displayed versus mass for three selected intervals of the relative azimuthal angle ϕ between the two pions.

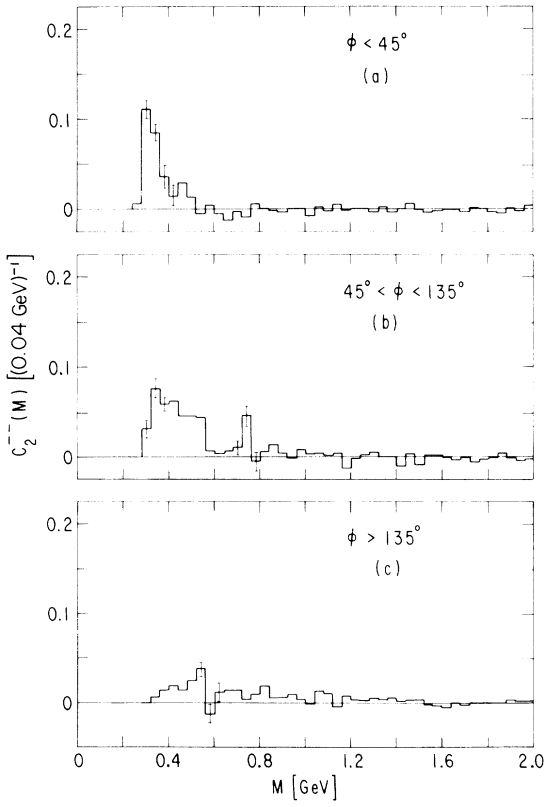

FIG. 4. As in Fig. 3, but for (− −) pairs.

vectors are parallel ($\phi = 0$). To display the result more clearly, and in an attempt to disentangle these kinematic biases, we present in Fig. 5 distributions of C_2 vs ϕ for pairs with $M < 0.42$ GeV. This interval is selected because it extends one pion mass above threshold and appears to include the principal structure seen in Fig. 4.

In Fig. 5(a), we observe that all three curves, ρ_2^{+-}, $\rho_1^+ \otimes \rho_1^-$, and C_2^{+-}, peak towards $\phi = 0$. Because the term $\rho_1^+(p_1)\rho_1^-(p_2)$ is uncorrelated in p_1 and p_2, the enhancement near $\phi = 0$ in this quantity at small M is purely kinematic. It arises, as explained above, because of the restriction of $M = (p_1 + p_2)^2$ to small values. The correlation function C_2^{+-} is nonzero in Fig. 5(a) for all ϕ. However, we note that the ratio $R^{+-} = C_2^{+-}/\rho_1^+ \otimes \rho_1^-$, tabulated in Table II, column 2, is nearly independent of ϕ. Its average value for $M \leq 0.42$ GeV is 0.64 ± 0.03. We conclude that dynamical correlation in ϕ, if present at small M, is not strong enough to overcome the strong kinematic influence. Of course, in doing this analysis, we have averaged over all p_T values and over the M range $0.28 < M < 0.42$ GeV. We cannot exclude the possibility that ϕ correlations may be observed in more differential distributions. Summarizing our result, we may write

$$C_2^{+-}(M, \phi) \simeq 0.64 \rho_1^+ \otimes \rho_1^-(M, \phi)$$

for

$$M < 0.42 \text{ GeV} .$$

In Fig. 5(b), the ϕ distributions for $(--)$ are shown for $M \leq 0.42$ GeV. Again, strong peaking towards $\phi = 0$ is observed in all three curves. In addition, the distribution ρ_2^{--} is suppressed near $\phi = 180°$. This suppression can also be observed in the ratio $R^{--} = C_2^{--}/\rho_1^- \otimes \rho_1^-$ (Table II).

As shown in Table II, column 3, the ratio is roughly constant at $R^{--} \simeq 0.45$ from $\phi = 0°$ to 120°, but then falls as $\phi \to 180°$. This behavior is *not* well represented by $a + b\cos\phi$ or some other simple form. Except for the clear depression near $\phi = 180°$, the $(--)$ correlation function seems to display no dynamical correlations in ϕ when averaged over p_T and $M < 0.42$ GeV.

We have also examined the ϕ dependence of $C_2(M, \phi)$ for pairs in the ρ mass band. These distributions are presented in Figs. 5(c) and 5(d), and ratios are tabulated in Table II, columns 4 and 5. Peaking towards $\phi = 180°$ is observed for the $(+-)$ case.

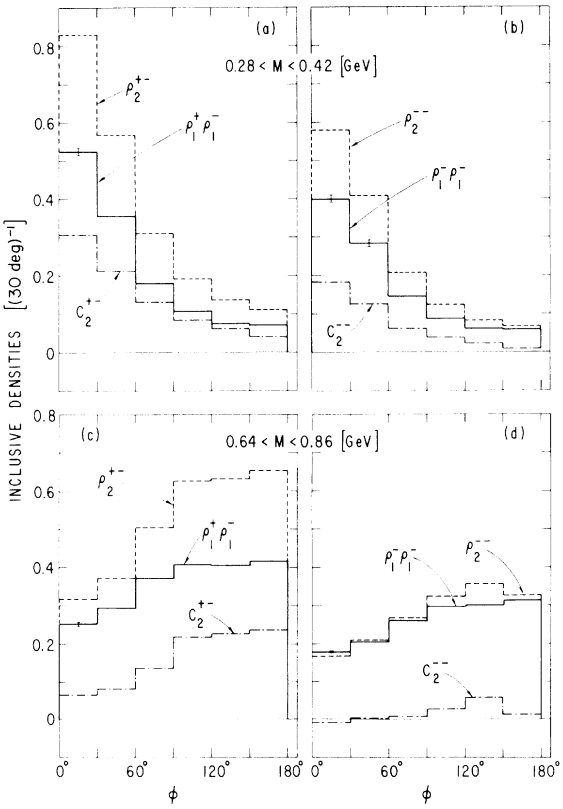

FIG. 5. The correlation function $C(M, \phi)$ versus ϕ for selected charged states and mass intervals:
(a) $+-$; $0.28 \leq M \leq 0.42$ GeV.
(b) $--$; $0.28 \leq M \leq 0.42$ GeV.
(c) $+-$; $0.64 \leq M \leq 0.86$ GeV.
(d) $--$; $0.64 \leq M \leq 0.86$ GeV.

III. PHENOMENOLOGICAL INTERPRETATION

In this section we discuss the interpretation of $C_2(M)$ from two complementary points of view. An analysis is given first in terms of the Mueller-Regge inclusive approach.[13] This is followed in Sec. III C by a description in terms of exclusive concepts.

A. Mueller-Regge model for $C_2(p_1, p_2)$

In the Mueller approach to inclusive correlations, the two-particle correlation function $C_2(p_1, p_2)$ is a properly defined discontinuity ("imaginary part")

TABLE II. Ratio $C_2/\rho_1 \otimes \rho_1$ as a function of azimuthal angle.

ϕ (deg)	$0.28 < M < 0.42$ GeV R^{+-}	R^{--}	$0.64 < M < 0.86$ GeV R^{+-}	R^{--}
0–30	0.58 ± 0.05	0.46 ± 0.05	0.26 ± 0.01	0.02 ± 0.02
30–60	0.60 ± 0.08	0.44 ± 0.07	0.27 ± 0.02	0.02 ± 0.01
60–90	0.73 ± 0.06	0.42 ± 0.05	0.36 ± 0.02	0.03 ± 0.02
90–120	0.79 ± 0.07	0.43 ± 0.05	0.53 ± 0.04	0.09 ± 0.02
120–150	0.82 ± 0.2	0.38 ± 0.15	0.56 ± 0.02	0.18 ± 0.02
150–180	0.57 ± 0.1	0.13 ± 0.07	0.57 ± 0.05	0.04 ± 0.03
All ϕ	0.64 ± 0.03	0.42 ± 0.03	0.45 ± 0.03	0.06 ± 0.01

of a four-particle-to-four-particle forward scattering amplitude.[13] At high energies, the Mueller-Regge approximation for $pp \to \pi\pi X$ is sketched in Fig. 6(a). This graph applies to dipion production in the central region of rapidity space.[14] The shaded oval represents a scattering amplitude from which the leading Pomeron exchange is excluded. We remark that the shaded oval does not represent the $\pi\pi$ elastic amplitude. Although the Pomerons are each attached to the oval at zero four-vector momentum, the structure of the oval is still that of an amplitude with six external legs. Consequently, there is no general reason to suppose that the dipion mass dependence of Fig. 6(a) should closely resemble that of elastic $\pi\pi$ scattering. In particular, in $C_2(M)$ for $pp \to \pi^+\pi^- X$, Fig. 6(a) leads us to expect resonance signals at the $\rho, f, g, \ldots$ positions, as well as a background. However, the relative contributions of the different resonant partial waves and the resonance-to-background ratio need not be related simply to those measured in studies of $\pi^+\pi^-$ elastic scattering. The data in Fig. 2 show in fact that the ρ resonance-to-background ratio in the M dependence of $pp \to \pi^+\pi^- X$ is much smaller than in the elastic $\pi^+\pi^-$ amplitude.

In an attempt to obtain a simple parametrization of the M dependence of $C_2(M)$ we study the behavior of Fig. 6(a) expected at large M, where a Regge-exchange approximation may be used. The resulting graphs are shown in Figs. 6(b) and 6(c) for $pp \to \pi^+\pi^- X$ and $pp \to \pi^-\pi^- X$, respectively. For $pp \to \pi^+\pi^- X$, the leading exchanged Reggeon R in Fig. 6(b) is the (ρ, f) pair, with intercept $\alpha_R(0) \simeq 0.5$. For $pp \to \pi^-\pi^- X$, more discussion is necessary.

In two-body phenomenology, duality arguments suggest that the Regge exchanges leading to an exotic system such as $\pi^-\pi^-$ occur in exchange-degenerate pairs, and that their contributions cancel in the imaginary part of the scattering amplitude. Applying analogous arguments to $pp \to \pi^-\pi^- X$, we expect that the exchange labeled E in Fig. 6(c) is either a low-lying trajectory or cut [e.g., $\alpha_E(0) \lesssim 0$] or a normal trajectory (e.g., α_ρ) whose small coupling at $t = 0$ is related to the deviation from exact exchange degeneracy. We admit parenthetically that the concept of an exchange contribution to the discontinuity of the forward amplitude may be altogether wrong in the case of the $\pi^-\pi^-$ channel, but we know of no other way to proceed.

B. Mass dependence of $C_2(p_1, p_2)$

Assuming that the exchanges in Figs. 6(b) and 6(c) are factorizable, we obtain the following limiting

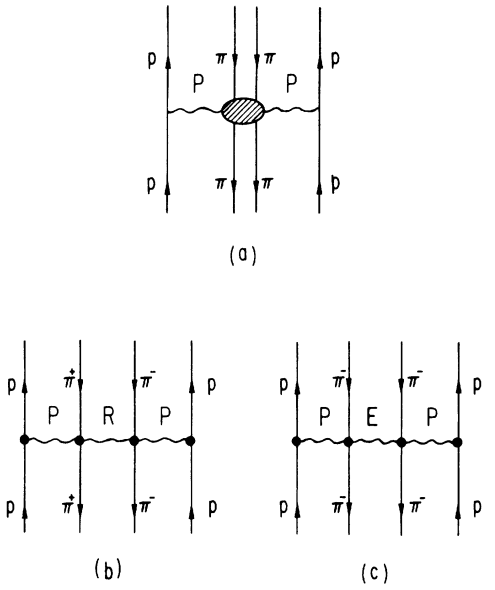

FIG. 6. (a) Mueller-Regge diagram for the inclusive reaction $pp \to \pi\pi X$ where the dipion system is produced in the central region of rapidity. The symbol P denotes the Pomeron. (b) Mueller-Regge diagram for $pp \to \pi^+\pi^- X$ at large s and large mass M of the $\pi^+\pi^-$ pair. (c) Mueller-Regge diagram for $pp \to \pi^-\pi^- X$ at large s and large mass M of the $\pi^-\pi^-$ pair.

expressions at large M:

$$C_2^{+-}(p_1, p_2) = \beta_{RP}(m_{T1})\beta_{RP}(m_{T2})(M^2)^{\alpha_R(0)-1} \propto M^{-1}, \text{ as } M \to \infty, \tag{3.1}$$

$$C_2^{--}(p_1, p_2) = \beta_{EP}(m_{T1})\beta_{EP}(m_{T2})(M^2)^{\alpha_E(0)-1}. \tag{3.2}$$

The transverse mass m_T is defined in Eq. (2.4); β_{RP} and β_{EP} are vertex functions whose m_T dependence may be estimated from data on the single-pion inclusive yield $\rho_1(p)$. In the central region, the Mueller-Regge approach provides the expansion

$$\rho_1(p) = \beta_{PP}(m_T) + \beta_{RP}(m_T)s^{-1/4}. \tag{3.3}$$

This equation shows that the vertex functions yield the transverse-momentum damping of $\rho_1(p)$.

As is apparent from Fig. 2, available data are concentrated at small M, where Eqs. (3.1) and (3.2) are not obviously applicable. Inasmuch as we are working with the imaginary parts of amplitudes, we might hope nevertheless that the extrapolation of Eqs. (3.1) and (3.2) to small mass is meaningful in the sense of a dual average. Since the ρ signal is not prominent in $C_2^{+-}(M)$, the average is not difficult to obtain.

We wish to compare Eqs. (3.1) and (3.2) with the data at low M and to extract effective values for

$\alpha_R(0)$ and $\alpha_E(0)$. The proper comparison should be done at fixed values of all kinematic variables other than M. Present statistics do not permit such a differential comparison. Integrating Eq. (3.1), we obtain

$$C_2^{+-}(M) = (M^2)^{\alpha_R(0)-1} \int\int dp_1 dp_2 \beta_{RP}(m_{T1}) \beta_{RP}(m_{T2}) \times \delta(M - [(p_1+p_2)^2]^{1/2}). \tag{3.4}$$

Here dp represents the invariant integration element d^3p/E. The integrations over the p_T and ϕ variables and over the longitudinal position of the dipion pair introduce an added dependence[15] on M through the δ function in Eq. (3.4).

It is a simple matter to show analytically that as $M \to 2m_\pi$, the integral in Eq. (3.4) provides a threshold suppression factor[16] proportional to $(M^2 - 4m_\pi^2)^{1/2}$. By contrast, at large M the transverse-momentum dependence of the vertex functions in Eq. (3.4) results in a function which falls rapidly with M. In order to extract the effective Regge power $\alpha_R(0)$ from the data on $C_2^{+-}(M)$, it is first necessary to divide out these important threshold and large-M factors. In the absence of a detailed knowledge of $\beta_{RP}(m_T)$, this procedure is necessarily approximative.

Returning to Eq. (3.3), we note that at large s the Mueller-Regge model provides the following prescription for the M dependence of the product $\rho_1^+ \otimes \rho_1^-$:

$$\rho_1^+ \otimes \rho_1^-(M) = \int\int dp_1 dp_2 \beta_{PP}(m_{T1}) \beta_{PP}(m_{T2}) \times \delta(M - [(p_1+p_2)^2]^{1/2}). \tag{3.5}$$

This integral has exactly the same form as that in Eq. (3.4), except for the replacement of $\beta_{RP}(m_T)$ by $\beta_{PP}(m_T)$. If we assume that the m_T dependences of β_{RP} and β_{PP} are identical, we may divide Eq. (3.4) by Eq. (3.5) to obtain

$$R^{+-}(M) \equiv \frac{C^{+-}(M)}{\rho_1^+ \otimes \rho_1^-(M)} \propto (M^2)^{\alpha_R(0)-1}. \tag{3.6}$$

Likewise,

$$R^{--}(M) \propto (M^2)^{\alpha_E(0)-1}. \tag{3.7}$$

Alternatively, assuming that β_{RP} in Eq. (3.1) has the same m_T dependence as β_{EP} in Eq. (3.2), we may work directly with Eq. (3.4) to derive

$$C_2^{--}(M)/C_2^{+-}(M) \propto (M^2)^{\alpha_E(0)-\alpha_R(0)}. \tag{3.8}$$

Motivated by Eq. (3.6), in Fig. 7 we display $R^{+-}(M)$ on a logarithmic scale. Beyond $M \simeq 2.5$ GeV the errors are large, and therefore we do not show the data. The form of Eq. (3.6) requires that the data points in Fig. 7 should fall on one straight line. Quite obviously they do not. An excursion is visible in the ρ region, as expected. For M values below the ρ position, a rough fit to the data suggests an effective trajectory with the rather high intercept $\alpha(0) \simeq 0.6$. For $M \gtrsim 1$ GeV, the intercept is much lower, $\alpha(0) \simeq 0.35$. In view of the approximations we have made, it is hazardous to propose strong conclusions. However, we call attention to the fact that the Mueller-Regge expectation of $\alpha(0) \simeq 0.5$ lies well within the range of values of $\alpha(0)$ which provide an acceptable average fit to the data in Fig. 7.

In Fig. 8, we display the ratio C_2^{--}/C_2^{+-} as suggested by Eq. (3.8). Here the statistics preclude an examination of the M dependence for $M \gtrsim 1$ GeV. For comparison, we show the M^{-2} dependence expected if $\alpha_R(0) - \alpha_E(0) = 1$ in Eq. (3.8). We observe that this form is consistent with the fall of C_2^{--}/C_2^{+-}. In the Mueller-Regge framework this result suggests that the process $pp \to \pi^-\pi^- X$ is mediated by a rather low-lying exchange, with intercept $\alpha_E(0) \simeq -0.5$. The duality expectation is borne out, in that the exchange-degenerate pair of ρ and f with intercept $\alpha(0) \simeq 0.5$ does not contribute to the M dependence of $pp \to \pi^-\pi^- X$. This result is an important verification that standard duality notions are applicable in inclusive processes. It stands in contrast to the list of embarassing failures associated with early scaling criteria.[13]

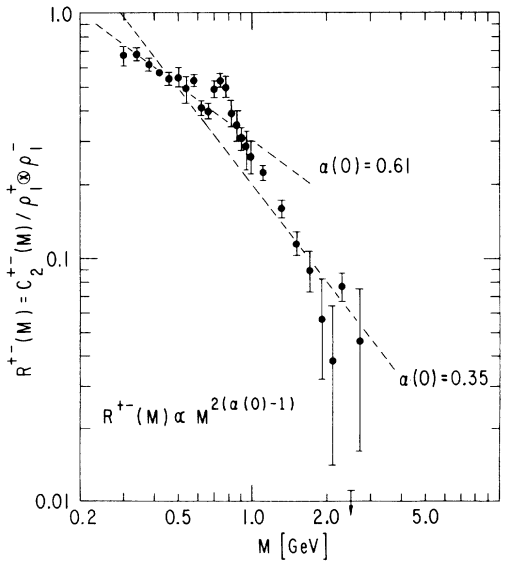

FIG. 7. The mass dependence of the ratio $R^{+-}(M) = C_2^{+-}(M)/\rho_1^+ \otimes \rho_1^-(M)$ for $pp \to \pi^+\pi^- X$ at 105 GeV/c. Two straight lines are drawn. They correspond to two choices of the parameter $\alpha(0)$ in the expression $R^{+-}(M) \propto (M^2)^{\alpha(0)-1}$ suggested by Mueller-Regge analysis.

In terms of rapidity, the Mueller-Regge expectation for the correlation function C^{--} is

$$C^{--}(\Delta y) \propto \exp\{[\alpha_E(0) - \alpha_P(0)]|\Delta y|\}. \quad (3.9)$$

The low intercept $\alpha_E(0) \simeq -0.5$ provides a correlation length $\lambda^{--} \equiv (\alpha_E - \alpha_P)^{-1} \simeq \frac{2}{3}$, much shorter than the $(+-)$ value $\lambda^{+-} \simeq 2$. The fact that $\lambda^{--} \simeq \frac{1}{3}\lambda^{+-}$ is to be contrasted with expectations of cluster models[4,5] in which typically $\lambda^{--} \simeq \lambda^{+-}$. Previously a small value of λ^{--} was suggested, on the basis of the observation[7] of a sharp peak near $\Delta y = 0$ in the rapidity variation of the two-dimensional distribution $C^{--}(\Delta y, \phi)$ *for values of* ϕ *near zero.* Our extraction of a small value of λ^{--} from the one-dimensional $C(M)$ is perhaps more direct. However, the two observations are surely related, since small M and small $(\Delta y, \phi)$ are correlated kinematically (cf. Sec. II C).

We turn now to an examination of the absolute magnitudes of $C_2^{+-}(M)$ and $C_2^{--}(M)$. The structure of Eq. (3.4) shows that

$$\frac{C_2^{--}(M)}{C_2^{+-}(M)} = \left(\frac{\bar{\beta}_{EP}}{\bar{\beta}_{RP}}\right)^2 M^{-2}. \quad (3.10)$$

In obtaining Eq. (3.10), we have defined vertex function $\bar{\beta}$ averaged over p_T and set $\alpha_R(0) - \alpha_E(0) = 1$. The data in Fig. 8 provide the estimate

$$\left(\frac{\bar{\beta}_{EP}}{\bar{\beta}_{RP}}\right)^2 \simeq \frac{1}{15} \quad \text{or} \quad \left|\frac{\bar{\beta}_{EP}}{\bar{\beta}_{RP}}\right| \simeq \frac{1}{4}.$$

We note that the exchange denoted E couples relatively weakly, at least in the imaginary part of the inclusive amplitude for $pp \to \pi^-\pi^- X$. Whether E is a factorizable singularity (or pair of singularities) which plays a role in the $\pi^-\pi^-$ elastic amplitude is open to question. However, presumably α_E does contribute to $pp \to \pi^+\pi^- X$ in much the same fashion as to $pp \to \pi^-\pi^- X$. Therefore, a consistent phenomenological study of $C_2^{+-}(M)$ would require a reanalysis of its M dependence in terms of both $\alpha_R(0)$ and $\alpha_E(0)$. The present data do not appear to warrant such a detailed treatment.

Turning to $pp \to \pi^+\pi^- X$, and using Eqs. (3.1) and (3.3)–(3.6), we may express $R^{+-}(M)$ as

$$R^{+-}(M) = \left(\frac{\bar{\beta}_{RP}}{\bar{\beta}_{PP}}\right)^2 (M^2)^{\alpha_R(0)-1}. \quad (3.11)$$

The data in Fig. 7 provide the estimate $(\bar{\beta}_{RP}/\bar{\beta}_{PP})^2 \simeq 0.25 \pm 0.05$. Recognizing that the trajectory R represents the (ρ, f) exchange-degenerate pair, whose couplings are presumed to be equal in magnitude, we deduce that

$$\left|\frac{\bar{\beta}_{fP}}{\bar{\beta}_{PP}}\right| \simeq \left|\frac{\bar{\beta}_{\rho p}}{\bar{\beta}_{PP}}\right| \simeq 0.35 \pm 0.04.$$

Fits to single-particle spectra[14,17] provide values of these ratios in the range 0.4 to 0.7. While these different estimates are in fairly close agreement, they suggest that $C_2^{+-}(M)$ is somewhat smaller (~50%) than expected in the Mueller-Regge framework on the basis of factorization and the properties of single-particle inclusive spectra.

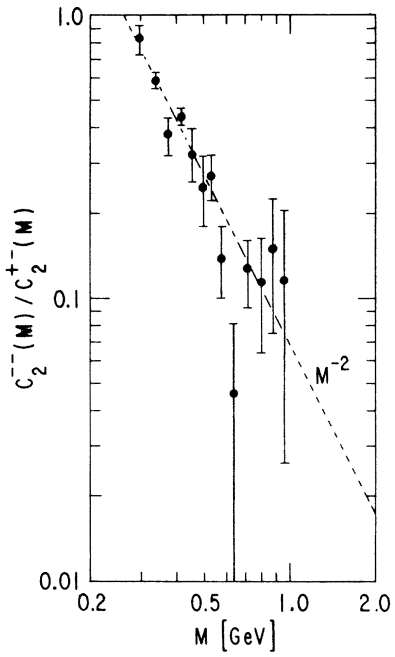

FIG. 8. The mass dependence of the ratio $C_2^{--}(M)/C_2^{+-}(M)$. The dashed line is drawn to show the M dependence expected if the ratio is proportional to M^{-2}. It is not a fit to the data.

As a final remark in this section, we comment on the energy dependence of $C_2(M)$. In all short-range-order models, $C_2(p_1, p_2)$ is expected to approach an energy-independent constant value as $s \to \infty$. This remains true if we integrate over all variables except M and $y_{\pi\pi}$. If the dipion system is distributed uniformly in rapidity, the integral over $y_{\pi\pi}$ is proportional to $\ln s$. Therefore, we may expect that $C_2^{\pm\pm}(M)/\ln s$ will become independent of s as $s \to \infty$. It would be useful to check this expectation with data at other energies.

C. Exclusive model for $C(M)$

To provide a second basis for understanding $C(M)$, we introduce an elementary exclusive phenomenological framework. We imagine that the production of pions occurs in several ways: They are produced singly, in correlated pairs, in correlated triplets, in correlated quartets, and so forth. For convenience, we use the term resonance to denote these correlated groups, although we have no evidence yet that all correlations are attributable to the resonances already

established. Borrowing from the vernacular, we qualify as "prompt" the mechanisms mentioned above: prompt single pions, prompt two-pion resonances, prompt three-pion resonances and so forth. The functions $G_1(p), G_2(p_1,p_2), G_3(p_1,p_2,p_3), \ldots$ stand for the densities of prompt single pions, two-pion resonances, three-pion resonances, ... produced in the high-energy interaction. They are symmetric functions of the momenta of their identical decay products. The single-particle density of observed pions is

$$\rho_1(p) = G_1(p) + \int dp_1 G_2(p,p_1) + \frac{1}{2!}\int dp_1 dp_2 G_3(p,p_1,p_2) + \cdots . \quad (3.12)$$

The integration dp in Eq. (3.12) is the invariant integration d^3p/E. Physically, Eq. (3.12) expresses the idea that the pions result from an incoherent sum of prompt single-pion production, as decay products of two particle resonances G_2, and so forth.

The mean multiplicity of pions is

$$\langle n_\pi \rangle = \int \rho_1(p) dp , \quad (3.13)$$

whereas the mean multiplicity of prompt pions is

$$\langle n_\pi \rangle_{\text{prompt}} = \int G_1(p) dp . \quad (3.14)$$

The two-pion correlation function is the sum of contributions from the prompt production of two pions, $G_2(p_1,p_2)$, plus the prompt production of three-pion resonances, integrated over the unobserved pion, and so forth. Explicitly,

$$C_2(p_1,p_2) = G_2(p_1,p_2) + \int dp_3 G_3(p_1,p_2,p_3) + \frac{1}{2!}\int dp_3 dp_4 G_4(p_1,p_2,p_3,p_4) + \cdots . \quad (3.15)$$

Likewise, the three-particle correlation function is expressed as

$$C_3(p_1,p_2,p_3) = \sum_{m=3} \frac{1}{(m-3)!}\int dq_1 \cdots dq_{m-3} G_m(p_1,p_2,p_3,q_1,\cdots q_{m-3}) . \quad (3.16)$$

A formal derivation of these results is given in Appendix B.

The correlation functions are determined by the prompt densities, which are the relative frequencies for direct production of an m-particle object. The first term in C_2, Eq. (3.15), is G_2, the density for prompt two-pion resonance production. The subsequent terms represent dipions which are decay products of the m-particle resonances, with $m \geq 3$. Removed from C_2 are all incoherent combinatorial backgrounds due to pions arising from different resonances.

By integrating G_2 over p_1 and p_2 we obtain the mean number of prompt pairs of correlated pions. Restricting the integral to the ρ-resonance region, we derive the mean number of prompt ρ mesons:

$$\langle n_\rho \rangle_{\text{prompt}} = \int_{\rho\ \text{region}} G_2(p_1,p_2) dp_1 dp_2 . \quad (3.17)$$

There are also ρ's among the decay products of m pion resonances ($m \geq 3$). The functions G_m ($m \geq 3$) provide a background of nonresonant $\pi^+\pi^-$ pairs in the ρ region as well. Consequently, in the vicinity of a particular two-pion resonance, such as the ρ, $C_2(M)$ is expected to have both a resonance and a background contribution. Unless all higher correlations are measured explicitly or otherwise parametrized, the resonance signal is obtained by the standard practice of fitting the data to the sum of background plus resonance functions, as was done in Sec. II B. The virtue of dealing with $C_2(M)$ rather than $\rho_2(M)$ is that the combinatorial background of pion pairs from different sources is eliminated from $C_2(M)$. Letting $B(p_1,p_2)$ stand for the background in C_2, we may express

$$\langle n_\rho \rangle = \int [C_2(p_1,p_2) - B(p_1,p_2)] dp_1 dp_2 . \quad (3.18)$$

Obviously the best way to study the properties of resonance production is to isolate the prompt functions G_m. This is difficult in exclusive final states unless one knows how many resonances are produced. The inclusive correlations provide a different method. Since each correlation function is linear in the prompt functions, knowledge of these correlations can be used to obtain the prompt densities.

The exclusive framework just developed provides us with certain qualitative expectations for the behavior of $C(M)$ as a function of mass. Peaks in $C^{+-}(M)$ should occur near the locations of known resonances, such as the ρ, f, and g. As explained, there will in general also be considerable background beneath the resonance peaks. The relative

magnitude of the resonance and background contributions in a given mass bin cannot be predicted unless we have a specific model for the prompt densities G_m. Third, in both $C^{--}(M)$ and $C^{+-}(M)$, we expect to observe a substantial enhancement just above threshold. If we take the full width of the A_1- and Q-meson signals as typical of the properties of threshold enhancements, we may suppose that the threshold structure in $C(M)$ will extend over a range of 200 to 400 MeV. This is consistent with the results shown in Fig. 2. These nonresonant threshold enhancements in $C(M)$ arise in part from the (integrals over the) G_m ($m \geq 3$) in Eq. (3.15). The nonresonant pairs of $\pi^+\pi^-$ and $\pi^-\pi^-$ from these G_m will tend to have small invariant mass (and thus be near threshold) simply because the G_m must yield pions whose momentum spectrum is peaked at small p_T and $x = 2p_L/\sqrt{s}$, as observed in the overall inclusive sample. Finally, superimposed on this broad threshold structure in the $\pi^-\pi^-$ distribution, there may be a discernable effect very near threshold due to Bose-Einstein symmetry requirements. We shall return to this question below.

We remark again that the model discussed here is necessarily qualitative. It is based on the assumption that pion production results from a sum of incoherent processes. It is a model for cross sections, not amplitudes, and we have ignored interference effects. Nevertheless, one conclusion which may be drawn directly from the data in Fig. 2 is that the bulk of the two-pion correlation arises from the decay of correlated states G_m of multiplicity $m \geq 3$. The two-pion resonances account for only ~10% of f_2^{+-}.

Through interference effects, the ρ meson may also induce a positive correlation in f_2^{--}. This can be understood heuristically by appeal to the Lovelace fit,[11] or by direct consideration of interference effects expected between multiparticle production *amplitudes*. We may postulate amplitudes for the production of prompt single pions and ρ's. The amplitude $A^{--}(p_1, p_2)$ for the production of two π^-'s must be properly symmetrized to satisfy Bose-Einstein statistics. In a specific model of this type,[18] it was found that a threshold peak is generated in $C_2^{--}(M)$. The integrated interference effect in f_2^{--} is roughly $0.5\ \langle n_{\rho 0}\rangle$. Taking the value $\langle n_{\rho 0}\rangle = 0.30 \pm 0.04$ determined in Sec. II, we conclude that about 20% of f_2^{--} may be a Bose-Einstein reflection of ρ production. Superposition and interference effects may be present in the $\pi^+\pi^-$ distribution also. In this case, isospin considerations provide the symmetrization requirement. Model estimates[18] suggest that about $0.25\langle n_{\rho 0}\rangle$ (only 4%) of the integrated low-mass enhancement may be explained in this way. For both $(+-)$ and $(--)$, the range of the interference effect extends one pion mass above threshold.

IV. CONCLUSIONS

We find that the correlation function in invariant mass is a useful way to display data from high-energy multiparticle processes. It reveals interesting structure not visible in rapidity. We observe strong positive correlations in both C_2^{+-} and C_2^{--} in the form of threshold peaks extending from the two-pion threshold to ≈ 0.6 GeV. In the $(--)$ combination this peak accounts for all of f_2^{--}; in the $(+-)$ combination it is responsible for 50% of f_2^{+-}. A ρ signal is visible above a broad background in $C_2^{+-}(M)$. For $M \leq 0.42$ GeV, we find no significant dynamical ϕ dependence in either $C_2^{+-}(M, \phi)$ or $C_2^{--}(M, \phi)$, except for a suppression near $\phi = 180^\circ$ in C_2^{--}. In examining the M dependence of $R^{--} = C_2^{--}/\rho_1^- \otimes \rho_1^-$, we find a rapid variation with M over the narrow range $0.28 < M < 0.42$ GeV. This variation is not inconsistent with Bose-Einstein effects. If present, the scale of this effect is about one pion mass.

The decrease of $C(M)$ as M increases is interpreted in the Mueller-Regge inclusive framework. For $C_2^{+-}(M)$, we find that the average M dependence is described by an effective trajectory with intercept $\alpha(0) \approx 0.5 \pm 0.1$, consistent with the expected (ρ, f) pair. For the exotic $(--)$ system, we find a low intercept, $\alpha(0) \approx -0.5$. These results support the application of standard duality concepts in inclusive processes. Correlations in the exotic $\pi^-\pi^-$ system are observed to be of much shorter range than those in $\pi^+\pi^-$. This important difference was not discernable in rapidity, where, in part because of the smearing introduced in converting M dependence into a y variation, similar correlation lengths are found for $(+-)$ and $(--)$ pairs.

In an exclusive framework, we relate most of the positive correlation in the low-M region to higher-mass resonances decaying into three or more pions. This picture could be checked by an examination of the mass dependence of the three-and-more-pion correlation functions.

ACKNOWLEDGMENT

We are indebted to the many physicists of the Argonne–Fermilab–Stony Brook collaboration for making these data available to us. E.L.B. is grateful to Dr. Vanna Cocconi for critical comments on an early draft of this article.

APPENDIX A: EXPERIMENTAL METHOD

To obtain $C_2(M)$, we must first evaluate the M dependence of the product $\rho_1 \otimes \rho_1$ of single-particle

spectra, Eq. (2.6). The single-particle distributions ρ_1 are determined experimentally both for positive (ρ_1^+) and for negative (ρ_1^-) particles. We compute the integrals in Eq. (2.6) by the Monte Carlo method. It is convenient to use as integration variables the longitudinal rapidities y_1 and y_2, the magnitude of the transverse momenta p_{T1} and p_{T2}, and the orientation angles ϕ_i of the transverse-momentum vectors. The single-particle density is a given function of y and p_T only. From y, p_T, and ϕ for each particle, the mass M is computed from Eq. (2.4).

Since the p_T distribution is exponentially damped we use importance sampling in the p_T integrations to increase the efficiency of the Monte Carlo procedure. To implement this, we make the substitution

$$\omega = \frac{1}{R^2}(1 - e^{-R^2 p_T^2}) . \tag{A1}$$

The p_T values in the data are limited to $p_T^2 \lesssim 1$ $(\mathrm{GeV}/c)^2$, so that ω has a maximum $\omega_0 \approx (1/R^2)$ $(1 - e^{-R^2})$. In terms of the new variables, the integral (2.6) is

$$\rho_1 \otimes \rho_1(M) = \int_{-Y/2}^{Y/2} dy_1 \int_0^{2\pi} d\phi_1 \int_0^{\omega_0} d\omega_1 \int_{-Y/2}^{Y/2} dy_2 \int_0^{2\pi} d\phi_2 \int_0^{\omega_0} d\omega_2 \, \tfrac{1}{4}\{\rho_1(p_1) e^{R^2 p_{T1}^2} \rho_1(p_2) e^{R^2 p_{T2}^2} \delta([(p_1+p_2)^2]^{1/2} - M)\}, \tag{A2}$$

where the curly-bracketed quantity is reexpressed in terms of (y_i, ϕ_i, ω_i). The value of R^2 is adjusted to make the bracketed quantity a slowly varying function of ω_i. The domain of the integrations in Eq. (A2) is a six-dimensional box which is populated uniformly.

There are two sources of uncertainty which contribute to the errors shown on the histograms of $C_2(M)$ in Figs. 1–5 and 7–8. First, there are the usual statistical and systematic experimental errors on ρ_2 and ρ_1. Second, there is an uncertainty introduced by the Monte Carlo integration method.

We estimate the total error on $\rho_2(M)$ by dividing the data sample into three equal parts. For each mass bin, the mean value and standard deviation of $\rho_2(M)$ are obtained by comparing results from the three subsamples. The central values and uncertainty of $\rho_1 \otimes \rho_1(M)$ are computed by generating several sets of Monte Carlo events and taking the average and standard deviation. The statistical error on $\rho_1 \otimes \rho_1(M)$ is negligible compared to the Monte Carlo error. The total uncertainty on $C_2(M)$ is the combination of the comparable independent errors on $\rho_2(M)$ and $\rho_1 \otimes \rho_1(M)$.

APPENDIX B: DERIVATION OF EQS. (3.12), (3.15), AND (3.16)

We adopt the specific interpretation of the prompt function G_m as an independent density for production of an m-particle resonance, which subsequently decays into pions, possibly through intermediate resonances. The cross section for a typical final state containing N resonances is

$$P_N^M = \int \frac{G_{m_1}^{n_1}}{m_1! n_1!} \frac{G_{m_2}^{n_2}}{m_2! n_2!} \cdots \frac{G_{m_N}^{n_N}}{m_N! n_N!} d^M p . \tag{B1}$$

The $M = m_1 n_1 + \cdots + m_N n_N$ distinct momentum labels are suppressed. We use G_m^n to denote $G_m(p_{11} \cdots p_{1m}) \cdots G_m(p_{n1} \cdots p_{nm})$. The integration $d^M p$ is the invariant integration over the M pion momenta. The cross section for making exactly M pions is

$$\sigma_M = \sum_N P_N^M . \tag{B2}$$

This is the sum of the cross sections (B1) over all possible numbers of produced resonances.

Generating-function techniques are a simple way of relating exclusive cross sections to inclusive cross sections.[19] For example, if one defines

$$\sigma(z) = \sum_M z^M \sigma_M , \tag{B3}$$

the integrals of the single-particle density and correlation functions are known to be

$$f_1 = \frac{\partial}{\partial z} \ln\sigma(z)\Big|_{z=1} ,$$
$$f_2 = \frac{\partial^2}{\partial z^2} \ln\sigma(z)\Big|_{z=1} , \tag{B4}$$
$$f_3 = \frac{\partial^3}{\partial z^3} \ln\sigma(z)\Big|_{z=1} .$$

For σ_M defined by (B2), using $M = \sum_i m_i n_i$, we

immediately derive

$$\sigma(z) = \exp\left(\sum_m \int d^m p \frac{G_m z^m}{m!}\right). \quad \text{(B5)}$$

A more sophisticated treatment allows z to be a function of the four-momentum p. Let z^m denote $z(p_1)\cdots z(p_m)$. Functional derivatives of $\ln\sigma(z(p))$ with respect to the function $z(p)$ yield the single-particle distribution, and n-particle correlation functions. Applying such functional derivatives to (B5) we obtain Eqs. (3.12), (3.15), and (3.16).

---

*Work performed under the auspices of the United States Energy Research and Development Administration.

†Work supported in part by the National Science Foundation.

[1]For recent summaries of high-energy correlation data, see L. Foa, Phys. Rep. 22C, 1 (1975); J. Whitmore, *ibid.* 10C, 273 (1974); and P. Darriulat, in Proceedings of the IV Colloquium on Multiparticle Dynamics, Oxford, 1975, edited by Chan Hong-Mo, R. Phillips, and R. Roberts [Rutherford Lab Report No. RL-75-143 (unpublished)].

[2]D. Amati, S. Fubini, and A. Stanghellini, Nuovo Cimento 26, 896 (1962); L. Bertocchi, S. Fubini, and M. Tonin, *ibid.* 25, 626 (1962).

[3]A. Mueller, Phys. Rev. D 2, 2963 (1972).

[4]E. L. Berger and G. C. Fox, Phys. Lett. 47B, 162 (1973); E. L. Berger, Nucl. Phys. B85, 61 (1975). The latter includes references to other literature on clusters.

[5]C. Quigg, P. Pirila, and G. Thomas, Phys. Rev. Lett. 34, 290 (1975); Phys. Rev. D 12, 92 (1975), and references therein; T. Ludlam and R. Slansky, *ibid.* 12, 59 (1975); 12, 65 (1975).

[6]ANL–Fermilab–Stony Brook collaboration: S. J. Barish *et al.*, Phys. Rev. D 9, 2689 (1974); Y. Cho *et al.*, Phys. Rev. Lett. 31, 413 (1973); R. Singer *et al.*, Phys. Lett. 49B, 481 (1974); T. Kafka *et al.* (unpublished).

[7]Aachen-CERN-Heidelberg-Munich ISR collaboration, K. Eggert *et al.*, Nucl. Phys. B86, 201 (1975); Michigan State–Argonne–Fermilab–Iowa State–Maryland collaboration, B. Y. Oh *et al.*, Phys. Lett. 56B, 400 (1975); G. A. Smith, paper presented at the Third International Winter Meeting on Fundamental Physics, Parador de Sierra Nevada, Spain, 1975 (unpublished).

[8]The structure in $C_2^{--}(M)$ in Fig. 2 near $M = 0.76$ GeV and that in $C_2^{+-}(M)$ near $M = 1.1$ GeV is statistically insignificant. Likewise, there is a one-bin fluctuation near $M = 0.76$ GeV in $C_2^{--}(M, \phi)$ in Fig. 4(b).

[9]Argonne–Stony Brook–Fermilab collaboration, R. Singer, T. H. Fields, L. Hyman, R. Engelmann, T. Kafka, M. Pratap, L. Voyvodic, R. Walker, and J. Whitmore, Phys. Lett. 60B, 385 (1976). Other recent papers on ρ production in high-energy collisions include Aachen-Berlin-Bonn-CERN-Cracow-Heidelberg-Warsaw collaboration, M. Deutschmann *et al.*, Nucl. Phys. B103, 426 (1976); F. C. Winkelmann *et al.*, Phys. Lett. 56B, 101 (1975); D. Fong *et al.*, *ibid.* 60B, 124 (1975).

[10]If we let the mass and width of the ρ vary in the fit, we determine $M_\rho = (749 \pm 1)$ MeV, $\Gamma = (105 \pm 18)$ MeV. This gives $\langle n_{\rho 0}\rangle = 0.28 \pm 0.06$ per inelastic event. The χ^2 is 12.6/(7 degrees of freedom).

[11]C. Lovelace, Phys. Lett. 28B, 265 (1968).

[12]G. Kopylov, Phys. Lett. 50B, 472 (1974); G. Cocconi, *ibid.* 49B, 459 (1974); Oh *et al.*, Ref. 7; Aachen-Berlin-Bonn-CERN-Cracow-Heidelberg-Warsaw collaboration, M. Deutschmann *et al.*, Nucl. Phys. B103, 198 (1976); A. Firestone *et al.*, *ibid.* B101, 19 (1975); N. N. Biswas *et al.*, Phys. Rev. Lett. 37, 175 (1976); J. Canter *et al.*, BNL Report No. BNL-20516, 1975 (unpublished); M. Pratap *et al.*, Phys. Rev. Lett. 33, 797 (1974).

[13]Mueller-Regge phenomenology has been quiescent of late. Various review articles may be consulted for introductory material: E.g., E. L. Berger, in *Proceedings of the II International Conference on Multiparticle Dynamics, Helsinki, 1971,* edited by E. Byckling, K. Kajantie, H. Satz, and J. Tuominiemi (Univ. of Helsinki, 1971); Chan Hong-Mo, in *Proceedings of the IV International Conference on High Energy Collisions, Oxford, 1972,* edited by J. R. Smith (Rutherford Laboratory, Chilton, Didcot, Berkshire, England, 1972).

[14]J. R. Freeman and C. Quigg, Phys. Lett. 47B, 39 (1973); S. Pinsky and G. Thomas, Phys. Rev. D 9, 1350 (1974).

[15]We remark that in working with Δy instead of M, one finds a similar extra Δy dependence in $C(\Delta y)$ at small Δy. The expression is

$$C^{+-}(\Delta y) \propto \int d^2p_{T1} \int d^2p_{T2}\, \beta(m_{T1})\beta(m_{T2})/M\,.$$

Only at large M and Δy, where $M^2 \sim m_{T1}m_{T2}\exp|\Delta y|$ does the p_T-dependent part of the integration factor, leading simply to $C^{+-}(\Delta y) \propto \exp(-\frac{1}{2}|\Delta y|)$.

[16]The importance of a threshold suppression was also noted by Cocconi (Ref. 12). We find that as $M \to 2m_\pi$, the threshold factor is proportional to $q = \frac{1}{2}(M^2 - 4m_\pi^2)^{1/2}$. In Ref. 12, it is stated that for $(M - 2m_\pi) \gg m_\pi$ the threshold factor is $\propto q^3$ for pions produced with no p_T damping. While we agree with this statement, we believe our factor of q is more appropriate very near threshold. The shape away from threshold depends strongly on the p_T damping.

[17]R. C. Brower, R. N. Cahn, and J. Ellis, Phys. Rev. D 7, 1080 (1973).

[18]G. Thomas, Argonne Report No. ANL-HEP-PR-76-33 (unpublished).

[19]A standard reference for generating-function techniques is A. H. Mueller, Phys. Rev. D 4, 150 (1970). The functions G_m used in the text are often termed cluster functions. We use instead the term "prompt" to avoid confusion because the word cluster has come to stand for many other things.